CHEMISTRY OF MATERIALS

ARTICLE

pubs.acs.org/cm

Low-Temperature Synthesis and HRTEM Analysis of Ordered Mesoporous Anatase with Tunable Crystallite Size and Pore Shape

Erik Nilsson,*,† Yasuhiro Sakamoto,‡ and Anders E.C. Palmqvist*,†

†Applied Surface Chemistry, Department of Chemical and Biological Engineering, Chalmers University of Technology, SE 412 96 Göteborg, Sweden

‡Nanoscience and Nanotechnology Research Center, Osaka Prefecture University, Sakai 599-8570, Japan

ABSTRACT: A new direct synthesis methodology for the preparation of mesoporous titania with hexagonal mesostructure and with walls of tunable crystallinity and crystallite size has been developed. As the crystallites grow they eventually reach a point where they are too big to fit within the pore walls, the mesoorder becomes distorted and is finally lost. It is run at an unprecedented low temperature of 40 °C without the need for an autoclave or high-temperature post-treatment procedures and is thus compatible with low temperature stable substrates. High-resolution transmission electron microscopy and electron diffraction reveal that the pore walls of the mesoordered material consists of anatase TiO_2 nanoparticles. The method allows for a wide choice of synthesis time during which the anatase crystallites grow slowly within the range of 2−5 nm in size but needs to be kept such that the crystallites have not yet grown too large for them to be coassembled into an ordered mesostructure.

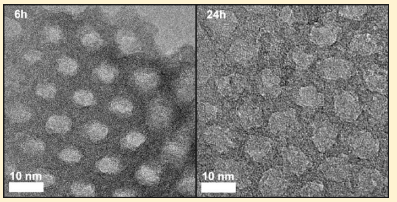

KEYWORDS: mesostructure, anatase, self-assembly, high-resolution electron diffraction, microemulsion, EISA

INTRODUCTION

In the early 1990's, a new family of porous inorganic materials with well-defined and regular pores in the meso-range was reported simultaneously by Kresge et al.[1,2] and Kurodas group.[3,4] The first syntheses of mesoordered materials reported were based on silica. These materials have received outstanding attention because of their various potential applications in areas such as separation technology, hosts for organic synthesis, heterogeneous catalysis etc. For advanced materials applications, e.g. involving electron transfer phenomena or magnetic interactions mesoordered materials based on other elemental compositions have become an important subject of research.[5−14]

Ordered mesoporous titania is of great interest for photophysical and photochemical applications due to their higher surface area, more uniform and controllable pore size and pore morphology, and superior interparticle connectivity compared to conventional randomly deposited nanoparticles of titania. The latter has been extensively studied for applications in dye-sensitized solar cells for electricity production, photocatalytic water splitting for hydrogen generation, and photocatalytic decomposition of contaminants in wastewater and air[15−20] and for these applications large specific surface areas and accessible pore structures are especially desirable. The merit of these materials has been found to depend largely on the intrinsic properties of titania, where the extent of crystallinity, polymorph type, particle size, and morphology are the most important parameters affecting materials performance.

The three main polymorphs of titania are brookite, anatase, and rutile, where the two latter are the most frequently used structures in titania-based solar energy conversion applications. Their photocatalytic activity has been debated and anatase has been suggested to be more photocatalytically active than rutile[17] but there are studies that show a similar or higher photocatalytic activity for rutile.[21−23] The photocatalytic activity of mesoordered anatase has been evaluated and found to be higher than for samples where the mesoorder was lost due to collapse induced by crystallite growth.[24] For ordered mesoporous titania materials to be useful here, it is hence a prerequisite for them to exhibit crystalline walls, preferably with tunable crystallite size and polymorph type, and a highly stable mesostructure.

Mesoordered materials are formed under wet chemical conditions in the presence of amphiphilic molecules as structure directing agents. This methodology requires the templating step of the synthesis to be made at low temperatures. The templating step is typically followed by a heat treatment step or a solvent extraction step where the templating agent is removed thus generating a mesoporous material. The crystallization of titania typically requires temperatures over 350 °C, and the transition from an as-prepared mesoordered amorphous titania to a crystalline is thus typically made through solid state reactions.[25,26] It has been shown that the mesoorder of titania in some cases is lost at temperatures as low as 250 °C for the hexagonal phase, whereas the cubic phase withstands 400 °C.[25] However, some hexagonal samples have been prepared stable up to 400 °C[26] and, when treated at 600 °C, while still maintaining hexagonal mesoorder found to undergo a drastic change in crystallite morphology to elongated particles.[27]

Thus, crystal growth through solid-state conversion is generally difficult to control in mesoordered materials as it tends to disrupt the mesoorder when the particles grow. For these reasons it is highly desirable to develop direct and low temperature

Received: December 17, 2010
Revised: April 12, 2011
Published: May 03, 2011

synthesis methods for ordered mesoporous titania. There have been some methods reported of mesoporous crystalline titania made at low temperatures.[28−32] Of these, only two methods show evidence of ordered mesoporosity,[28,29,33] the first involves formation of mesoordered anatase from a sol−gel reaction of $TiOSO_4$ in the presence of the cationic surfactant CTAB at 60 °C for an optimum duration, whereas the second utilizes an autoclave treatment of a butanolic solution of the triblock copolymer Pluronic P123 as structure directing agent and titanium butoxide as precursor. Both methods are promising, but whereas the first is limited in achievable anatase crystallite size to 1 nm, above which the mesoorder collapses, the second uses higher temperature and offers lower control over crystal growth due to the use of an autoclave.

In parallel, we have developed low-temperature microemulsion-mediated synthesis methods for suspensions of high specific surface area titania nanoparticles using various surfactant systems, and most recently we showed it possible using a microemulsion based on the nonionic triblock copolymer Pluronic F127.[23,34,35] In this system, the crystalline structure of TiO_2 can be controlled by varying the temperature and molar composition of the synthesis mixture. By judicious choice of synthesis conditions either rutile or anatase can be prepared in this microemulsion system. Which polymorph that forms depends on the particle nucleation and growth kinetics, and the thermodynamics of the synthesis reaction. These parameters depend specially on synthesis temperature, type of acid used, and surfactant. The combination of synthesis temperature used and molar composition of the reaction solution controls the relative rates of formation of the different polymorphs. Because of differences in rate-determining activation energies the rates of formation of different TiO_2 polymorphs may also have different temperature dependencies. The large number of possible combinations of synthesis parameters in this system allows for a highly controlled synthesis of nanoparticulate crystalline TiO_2.[35] The system is also very interesting from the perspective of mesostructured materials synthesis since it exhibits large regions in its phase diagram where liquid crystalline phases are stable[36] and this can be used for preparation of mesostructured materials. Here, we show a new synthesis route to mesoordered anatase based on a modification of the microemulsion route that offers tunable crystallite size within a permitting range and is carried out at 40 °C without autoclave.

EXPERIMENTAL SECTION

The chemicals used in this study were the nonionic ethyleneoxide$_{100}$-propyleneoxide$_{70}$-ethyleneoxide$_{100}$ triblock copolymer Pluronic F127, M_w 12600 g/mol (SIGMA), titanium(IV)butoxide (97% Aldrich), 1-butanol ≥99.4% (SIGMA-Aldrich), hydrochloric acid 37% (SIGMA-Aldrich). A clear solution containing HCl, Pluronic F127 and ethanol was prepared. To this solution titanium(IV)butoxide was added dropvise until the final mixture contained the weight proportions of 1:1.5:2:1 of 5 M acid:F127:ethanol:Ti(IV)$(BuO)_4$. The proportions were based on the binary F127-water phase diagram targeting the hexagonal phase.[36] Samples were drawn from the mixture at different time periods ranging from 3 h to 48 h and spin-coated (SPIN150 wafer spinner) on glass substrates in a two-step procedure starting at 300 rpm for 5 s followed by 1000 rpm for 10 s.

The deposited films were aged for at least 2 days at ∼20 °C in a closed chamber, also containing a separate container of saturated NaCl-solution open to air in order to keep the humidity in the chamber high and constant. The polymer template was finally removed from the film by irradiation with UV light in a closed chamber for 1 day during which the polymer is photocatalytically combusted.

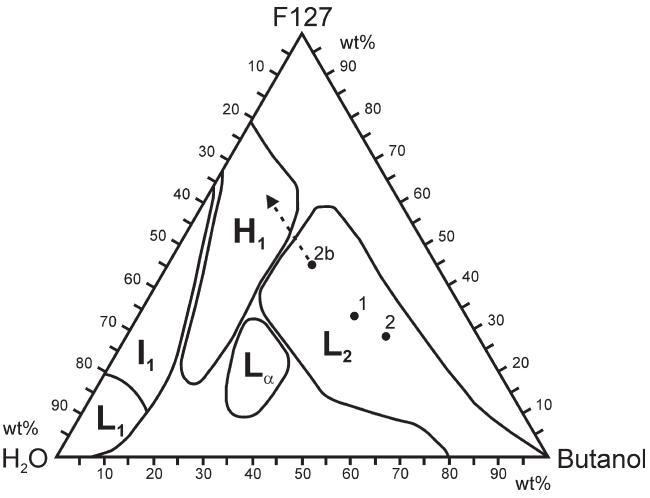

Figure 1. Gradual change in composition of the synthesis mixture within the phase diagram during synthesis. The ternary phase diagram is redrawn from Holmqvist et al.[36] Position 1 represents initial composition of reaction mixture. Position 2 represents composition of reaction mixture after hydrolysis of the alkoxide. Position 2b represents composition after evaporation of ethanol and prior to evaporation of butanol and water. Dotted line illustrates expected path of compositional change during evaporation of butanol and water.

High-resolution TEM observations were performed using a JEOL JEM-3010 operating at 300 kV (Cs = 0.6 mm, point resolution 1.7 Å). Images and electron diffraction patterns were recorded with a CCD camera (MultiScan model 749, Gatan, 1024 × 1024 pixels, pixel size 24 μm) and/or films. For the TEM analysis the samples were crushed in an agate mortar, dispersed in ethanol and dropped onto a microgrid. The microgrid had in advance been coated with gold before sample preparation, where the gold acts as an internal standard to calibrate the camera length for the electron diffraction patterns.

RESULTS AND DISCUSSION

In the initial step of the synthesis method developed here, nanocrystallites of anatase form and grow slowly in a microemulsion based on the triblock copolymer F127, hydrochloric acid, butanol and ethanol. The ethanol is assumed to act as an oil-phase together with butanol and since the initial mixture is transparent and nonphase-separating it represents a reversed micellar phase. The gradual change of the composition of the synthesis mixture in the phase diagram during synthesis can be followed in Figure 1. Initially the composition of the synthesis mixture is at position (1) in the phase diagram. As butanol forms during the hydrolysis of the alkoxide, the composition of the mixture in the phase diagram shifts to position (2). Positions (1) and (2) are thus the extreme-points of the reaction condition during the hydrolysis and condensation step. In this region of the phase-diagram the nanocrystallites are formed and grow slowly and to desired size as the mixture is aged at 40 °C in a closed polypropylene vessel for the duration of choice suitable for the desired crystallite size. After reaching the desired size the anatase crystallites are subsequently arranged in a coassembly process with the polymer forming a liquid crystalline inorganic/organic composite during the spin-coating procedure according to the evaporation induced self-assembly concept.[37] The reaction

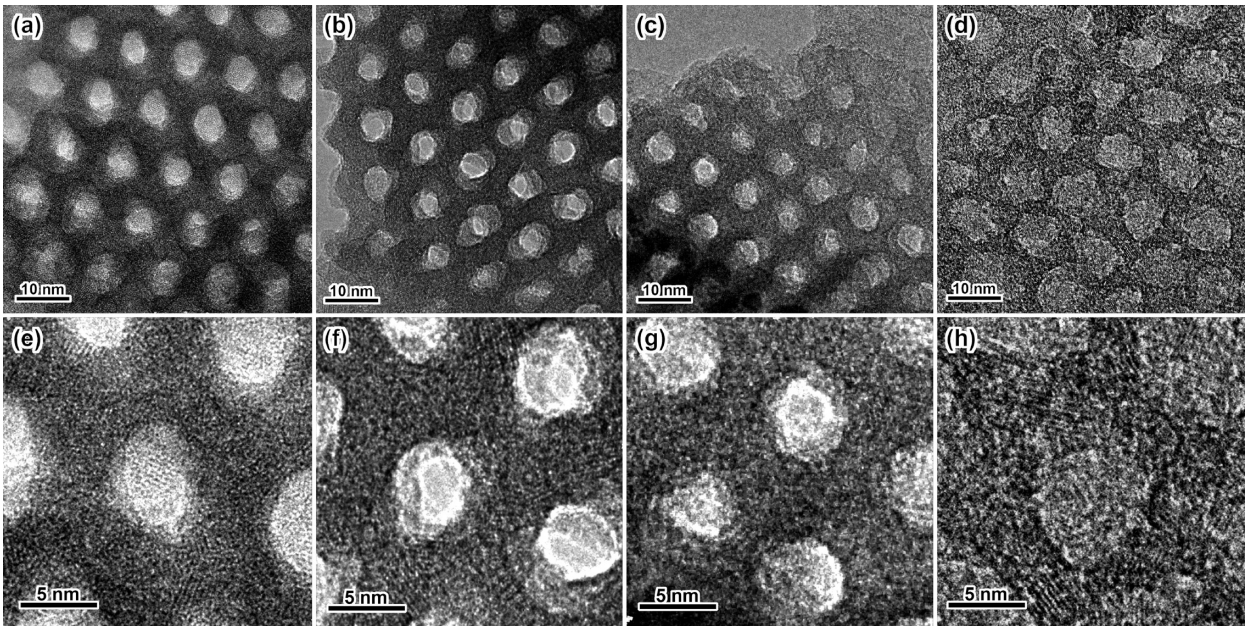

Figure 2. High-resolution TEM images of mesoporous TiO_2 prepared at different reaction times amounting to (a, e) 3, (b, f) 6, (c, g) 12, and (d, h) 24 h. Images e−h show the magnified images of TEM images a−d, illustrating the effects of synthesis time on mesostructure. The hexagonally arranged mesopore structure formed at 3 h remained up to 24 h where the pores became distorted.

solution is deposited as a thin film on a substrate allowing the solvent to evaporate and inducing formation of the liquid crystal at an appropriate choice of time where the crystallites have grown to their desired size but are not yet too large for the coassembly process to yield the desired mesostructure. Following deposition of the films the solvent evaporates, which shifts the composition of the mixture. The ethanol, which is added to lower the viscosity of the solution and thus facilitate the later film formation step, is expected to evaporate first of the solvents present and thus shifts conditions closer to the boundary between the H_1- and the L_2-phases to position (2b) in Figure 1. Evaporation of additional solvents increases the surfactant concentration thus facilitating formation of the liquid crystal (dotted line). However, the exact final composition is hard to estimate because of the equilibrium humidity between the air and film. The liquid crystal now serves as a template for the mesoordered walls of titania.

This facile and tunable method is compatible with low-temperature stable support materials such as polymers since it does not require temperatures over 40 °C. Interestingly, we find that the thermal stability of the final material is notably high compared to similar materials prepared by other methods.[24,25] The mesoorder remains intact also after treating the material thermally at 450 °C for 2 h using a heating rate of 10 °C/min. We hypothesize that this is due to lower stress levels in the material prepared by assembly of ready-made nanoparticles than via crystallization of as-prepared amorphous mesoporous titania in earlier work. Below follows a detailed analysis of the effects of the duration of the crystal growth employed on the materials prepared.

Effects of Synthesis Time on Mesostructure. A series of samples was prepared differing in duration of treatment in the microemulsion and thus in the time allowed for crystal growth ranging from 3 to 48 h. The prepared films were characterized using high resolution transmission electron microscopy and Figure 2 shows the time dependence of the sample series except for the 48 h sample. All samples shown exhibit a hexagonally ordered meso-structure of titania with a pore size of ca. 5 nm and with ca. 5 nm thick walls, apparently similar for samples made at 3, 6, and 12 h. The walls consist partially of nanosized TiO_2 crystals with several nanometers in size and with a size that increases with synthesis duration among these three samples. The sample prepared at 24 h synthesis time shows, however, mesopores that have become distorted and expose irregular shapes with inhomogeneous wall thickness but with a more crystalline wall than the earlier samples. The sample prepared after 48 h does not display a regular mesoorder and is not shown here. These results are in excellent agreement with our recent study of the formation of nanocrystalline TiO_2 within these time scales in a similar but compositionally somewhat different system.[35] For the conditions employed it is expected that crystalline nanoparticles form in the first stage and undergo a coassembly process with the liquid crystal-forming block copolymer, during which they become incorporated in the pore wall of the mesostructure together with some unreacted amorphous titania, which partakes in the cross-linking of the nanocrystallites in the wall matrix. This theory is supported by the series of high-resolution TEM images of the spincoated samples shown in Figure 2e−h. From these micrographs lattice fringes of TiO_2 crystals are evident within the pore walls, and the areas showing such fringes increase with synthesis time. For the sample prepared during 24 h of synthesis it becomes evident that large crystallites or aggregates of crystallites are not fully compatible with an ordered arrangement of mesopores when they are too large to fit within the walls of the mesostructure. This phenomenon explains the gradual loss of mesoorder seen in Figure 2a−d.

Effects of Synthesis Time on Atomic Order. The atomic order of the formed crystallites was evaluated by means of electron diffraction (ED). Figure 3 shows TEM images and ED patterns of the mesoporous TiO_2 samples prepared with the synthesis times of 3 h, 12 h and 48 h illustrating the meso-ordered pore structure and Debye−Scherrer rings due to the polycrystalline atomically ordered structure, respectively. To characterize the

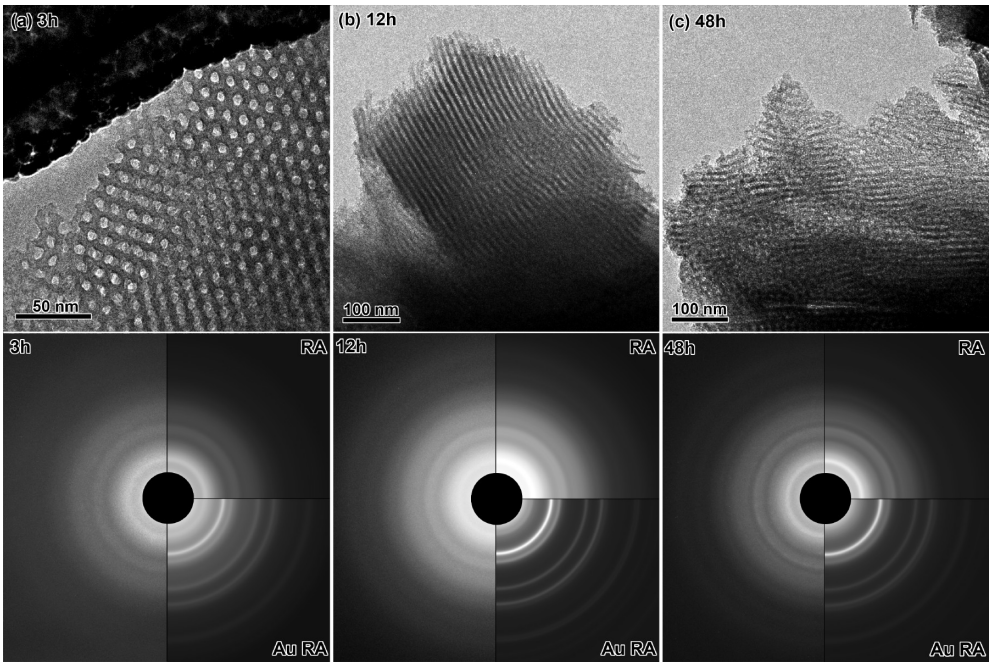

Figure 3. Low-magnification TEM images of mesoporous TiO_2 prepared at different reaction times of (a) 3, (b) 12, and (c) 48 h. The bottom part shows the electron diffraction (ED) patterns of each sample divided in three parts. Images show ED patterns (left) and rotational averaged ED patterns (right-top) of the mesoporous TiO_2, and the rotational averaged ED patterns of sputtered gold for calibration (right-bottom).

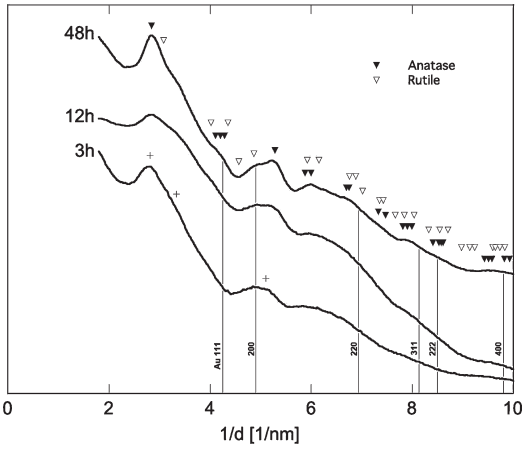

Figure 4. Profiles of the rotational averaged ED patterns of mesoporous TiO_2 prepared with the synthesis time of 3, 12, and 48 h as shown in Figure 3. The camera lengths were calibrated by a gold standard sputtered on the carbon microgrid for TEM observation. The peak positions of gold are also shown.

atomic order of the samples, the intensity profiles of the rotationally averaged (RA) ED patterns have been collected and are shown in the right-top of the ED pattern. The camera length was calibrated by an internal standard consisting of gold sputtered onto the TEM grids (right-bottom of the rotationally averaged ED pattern, Au RA).

Figure 4 shows the intensity profiles of the ED patterns, which are plotted versus the inverse of the *d*-spacing. The profile of the mesoporous TiO_2 with the synthesis time of 3 h shows several broad peaks, around 2.8, 5.0, and 6.2 nm^{-1}. The first peak exposes an additional small bump at a larger value of $1/d$, both of which are marked with + in Figure 4. These can be assigned to Ti−Ti distances of vertex-shared TiO_2 octahedra ($d = 0.355$ nm, $1/d = 2.82$ nm^{-1}) and edge shared TiO_2 octahedra ($d = 0.300$ nm, $1/d = 3.33$ nm^{-1}), respectively. The second peak, which is also marked with a + in Figure 4, corresponds to the Ti−O distance in the sample and has a value of $d = 0.196$ nm and $1/d = 5.10$ nm^{-1}. These peaks may originate from an amorphous structure of TiO_2 including small nanocrysallites with the size of ca. 2−3 nm.

The mesoporous TiO_2 sample prepared at 12 h of synthesis time shows more or less the same profile as that of 3 h, whereas the mesoporous TiO_2 sample prepared at 48 h, which has a less mesoordered and less mesoporous structure, shows clearer peaks in Figure 4. These peaks can be assigned to the anatase structure rather than the rutile structure. The first peak is present around $1/d = 2.9$ nm^{-1} and is assigned to the (101) reflection of anatase structure, marked by a solid triangle in Figure 4. Also the other reflections at larger 1/d values appear in good agreement with anatase, and together with the peaks due to the gold standard they explain the profile very well.

Besides the synthesis time other factors such as temperature, acid type, and acid strength have been found to be of key importance for titania syntheses in microemulsions.[23,34,35] These are also of similar importance when developing syntheses for mesostructured titania and in addition to these, the composition of the microemulsion, the state of the alkoxide precursor and the humidity of the air will all affect the outcome of the synthesis.[38] It should therefore be expected that small variations in these and similar synthesis conditions will affect the crystal structure of the TiO_2 as well as the mesostructure of the prepared films.

CONCLUSIONS

A new direct synthesis methodology for the preparation of mesoporous titania with hexagonal mesostructure and with walls of tunable crystallinity and crystallite size has been developed

dx.doi.org/10.1021/cm103600q |*Chem. Mater.* 2011, 23, 2781–2785

whereby the comparably thick walls of the material allow for particle sizes up to 5 nm to be integrated in the walls with retained mesoorder. The synthesis is done without the need of an autoclave and is done at an unprecedented low temperature of 40 °C using a modified microemulsion based method combined with the evaporation induced self-assembly process. A series of syntheses was performed and followed over synthesis time between 3 and 48 h, whereby the size of the final anatase crystallites could be varied within the range of ca. 2−5 nm. Already at an early stage the mesopores of the formed material appeared well-ordered in a hexagonal pattern. As the crystallites grow they eventually reach a point where they are too big to fit within the pore walls. At this point the pores become distorted and at still longer synthesis times the mesoorder is finally lost. The anatase structure of the crystalline pore walls was confirmed by electron diffraction. Because of the similarities with microemulsion-based methods for synthesis of suspensions of titania nanocrystals, we propose that additional mesostructures and titania polymorphs could be made by proper adjustment of the synthesis parameters available. In addition, the methodology is expected to be generally applicable to any material that can be prepared as nanoparticles in microemulsion systems.

AUTHOR INFORMATION

Corresponding Author

*E-mail: erik.nilsson@chalmers.se (E.N.); anders.palmqvist@chalmers.se (A.E.C.P). Fax: +46 31 16 00 62 (E.N.); +46 31 16 00 62 (A.E.C.P). Phone: +46 31 7722957 (E.N.); +46 31 7722961 (A.E.C.P).

ACKNOWLEDGMENT

E.N. thanks the National Graduate School in Material Science and the Foundation for Strategic Research for financial support. A.E.C.P. thanks the Swedish Research Council for financial support of a Senior Researcher position.

REFERENCES

(1) Kresge, C. T.; Leonowicz, M. E.; Roth, W. J.; Vartuli, J. C.; Beck, J. S. *Nature* **1992**, *359*, 710.
(2) Beck, J. S.; Vartuli, J. C.; Roth, W. J.; Leonowicz, M. E.; Kresge, C. T.; Schmitt, K. D.; Chu, C. T. W.; Olson, D. H.; Sheppard, E. W.; Mccullen, S. B.; Higgins, J. B.; Schlenker, J. L. *J. Am. Chem. Soc.* **1992**, *114*, 10834.
(3) Yanagisawa, T.; Shimizu, T.; Kuroda, K.; Kato, C. *Bull. Chem. Soc. Jpn.* **1990**, *63*, 988.
(4) Inagaki, S.; Fukushima, Y.; Kuroda, K. *J. Chem. Soc. Chem. Commun.* **1993**, 680.
(5) Antonelli, D. M.; Ying, J. Y. *Chem. Mater.* **1996**, *8*, 874.
(6) Templin, M.; Franck, A.; DuChesne, A.; Leist, H.; Zhang, Y. M.; Ulrich, R.; Schadler, V.; Wiesner, U. *Science* **1997**, *278*, 1795.
(7) Tian, Z. R.; Tong, W.; Wang, J. Y.; Duan, N. G.; Krishnan, V. V.; Suib, S. L. *Science* **1997**, *276*, 926.
(8) Attard, G. S.; Bartlett, P. N.; Coleman, N. R. B.; Elliott, J. M.; Owen, J. R.; Wang, J. H. *Science* **1997**, *278*, 838.
(9) Ulagappan, N.; Rao, C. N. R. *Chem. Commun.* **1996**, 1685.
(10) Sayari, A.; Liu, P. *Microporous Mater.* **1997**, *12*, 149.
(11) Yang, P. D.; Zhao, D. Y.; Margolese, D. I.; Chmelka, B. F.; Stucky, G. D. *Nature* **1998**, *396*, 152.
(12) Lee, J. K.; Kim, G. P.; Song, I. K.; Baeck, S. H. *Electrochem. Commun.* **2009**, *11*, 1571.
(13) Pokhrel, S.; Simion, C. E.; Teodorescu, V. S.; Barsan, N.; Weimar, U. *Adv. Funct. Mater.* **2009**, *19*, 1767.
(14) Liu, Q.; Zhang, W. M.; Cui, Z. M.; Zhang, B.; Wan, L. J.; Song, W. G. *Microporous Mesoporous Mater.* **2007**, *100*, 233.
(15) Oregan, B.; Grätzel, M. *Nature* **1991**, *353*, 737.
(16) Fujishima, A.; Honda, K. *Nature* **1972**, *238*, 37.
(17) Hoffmann, M. R.; Martin, S. T.; Choi, W. Y.; Bahnemann, D. W. *Chem. Rev.* **1995**, *95*, 69.
(18) Hagfeldt, A.; Boschloo, G.; Sun, L. C.; Kloo, L.; Pettersson, H. *Chem. Rev.* **2010**, *110*, 6595.
(19) Osterloh, F. E. *Chem. Mater.* **2008**, *20*, 35.
(20) Malato, S.; Blanco, J.; Vidal, A.; Richter, C. *Appl. Catal., B* **2002**, *37*, 1.
(21) Kim, S. J.; Lee, H. G.; Kim, S. J.; Lee, J. K.; Lee, E. G. *Appl. Catal., A* **2003**, *242*, 89.
(22) Sun, J.; Gao, L.; Zhang, Q. H. *J. Am. Ceram. Soc.* **2003**, *86*, 1677.
(23) Andersson, M.; Österlund, L.; Ljungstrom, S.; Palmqvist, A. *J. Phys. Chem. B* **2002**, *106*, 10674.
(24) Andersson, M.; Birkedal, H.; Franklin, N. R.; Ostomel, T.; Boettcher, S.; Palmqvist, A. E. C.; Stucky, G. D. *Chem. Mater.* **2005**, *17*, 1409.
(25) Alberius, P. C. A.; Frindell, K. L.; Hayward, R. C.; Kramer, E. J.; Stucky, G. D.; Chmelka, B. F. *Chem. Mater.* **2002**, *14*, 3284.
(26) Choi, S. Y.; Mamak, M.; Coombs, N.; Chopra, N.; Ozin, G. A. *Adv. Funct. Mater.* **2004**, *14*, 335.
(27) Choi, S. Y.; Mamak, M.; Speakman, S.; Chopra, N.; Ozin, G. A. *Small* **2005**, *1*, 226.
(28) Haseloh, S.; Choi, S. Y.; Mamak, M.; Coombs, N.; Petrov, S.; Chopra, N.; Ozin, G. A. *Chem. Commun.* **2004**, 1460.
(29) Shibata, H.; Ogura, T.; Mukai, T.; Ohkubo, T.; Sakai, H.; Abe, M. *J. Am. Chem. Soc.* **2005**, *127*, 16396.
(30) Shieh, D. L.; Li, J. S.; Shieh, M. J.; Lin, J. L. *Microporous Mesoporous Mater.* **2007**, *98*, 339.
(31) Sakai, T.; Yano, H.; Ohno, M.; Shibata, H.; Torigoe, K.; Utsumi, S.; Sakamoto, K.; Koshikawa, N.; Adachi, S.; Sakai, H.; Abe, M. *J. Oleo Sci.* **2008**, *57*, 629.
(32) Kao, L. H.; Hsu, T. C.; Cheng, K. K. *J. Colloid Interface Sci.* **2010**, *341*, 359.
(33) Shibata, H.; Mihara, H.; MLikai, T.; Ogura, T.; Kohno, H.; Ohkubo, T.; Sakait, H.; Abe, M. *Chem. Mater.* **2006**, *18*, 2256.
(34) Andersson, M.; Kiselev, A.; Österlund, L.; Palmqvist, A. E. C. *J. Phys. Chem. C* **2007**, *111*, 6789.
(35) Nilsson, E.; Furusho, H.; Terasaki, O.; Palmqvist, A. E. C. *J. Mater. Res.* **2011**, *26*, 1.
(36) Holmqvist, P.; Alexandridis, P.; Lindman, B. *J. Phys. Chem. B* **1998**, *102*, 1149.
(37) Brinker, C. J.; Lu, Y.; Sellinger, A.; Fan, H. *Adv. Mater.* **1999**, *11*, 579.
(38) Soler-illia, G. J. D.; Sanchez, C.; Lebeau, B.; Patarin, J. *Chem. Rev.* **2002**, *102*, 4093.